

## String junctions in flag manifold sigma model

---

Yuki Amari<sup>a</sup> Toshiaki Fujimori<sup>b,a</sup> Muneto Nitta<sup>a,c</sup> and Keisuke Ohashi<sup>a</sup>

<sup>a</sup>*Department of Physics & Research and Education Center for Natural Sciences, Keio University, 4-1-1 Hiyoshi, Kanagawa 223-8521, Japan*

<sup>b</sup>*Department of Fundamental Education, Dokkyo Medical University, 880 Kitakobayashi, Mibu, Shimotsuga, Tochigi 321-0293, Japan*

<sup>c</sup>*International Institute for Sustainability with Knotted Chiral Meta Matter(SKCM<sup>2</sup>), Hiroshima University, 1-3-2 Kagamiyama, Higashi-Hiroshima, Hiroshima 739-8511, Japan*

*E-mail:* [amari.yuki@keio.jp](mailto:amari.yuki@keio.jp), [toshiaki.fujimori018@gmail.com](mailto:toshiaki.fujimori018@gmail.com),  
[nitta@phys-h.keio.ac.jp](mailto:nitta@phys-h.keio.ac.jp), [keisike084@gmail.com](mailto:keisike084@gmail.com)

ABSTRACT: We numerically construct a stable three-string junction of Y-shape in a flag manifold nonlinear sigma model on  $SU(3)/U(1)^2$ .

---

## Contents

<b>1</b>	<b>Introduction</b>	<b>1</b>
<b>2</b>	<b><math>F_{N-1}</math> Faddeev-Skyrme model</b>	<b>3</b>
2.1	The model	3
2.2	Topological lump strings	4
<b>3</b>	<b>BPS lump solutions as initial configurations</b>	<b>5</b>
3.1	Non-Kähler and Kähler $F_{N-1}$ sigma models	5
3.2	BPS lumps in the $F_2$ sigma model on $T^2$	7
<b>4</b>	<b>Numerical solution of string junctions</b>	<b>8</b>
4.1	Initial configuration and boundary condition	8
4.2	Numerical results	10
<b>5</b>	<b>Summary and Discussion</b>	<b>11</b>
<b>A</b>	<b>Parametrization of the Lagrangian</b>	<b>13</b>
<b>B</b>	<b><math>F_{N-1}</math> sigma model with general coefficients</b>	<b>15</b>
<b>C</b>	<b>Numerical calculation</b>	<b>16</b>
C.1	$F_{N-1}$ on the lattice	16
C.2	Numerical method and some results	17

---

## 1 Introduction

Color confinement in quantum chromodynamics (QCD) is one of the most challenging problems in modern physics. Quarks are confined by color electric flux tubes called confining strings. Consequently, particles observed in nature are hadrons; mesons are bound states of a quark and an anti-quark confined by a string, while baryons consist of three quarks confined by three strings possibly joined at a junction. Taking a duality, confining strings are mapped to  $\mathbb{Z}_N$  vortices in which magnetic fluxes are confined, and quarks are mapped to monopoles. Thus, monopoles and anti-monopoles are confined by color magnetic flux tubes as a dual Meissner effect [1, 2]. When one pulls a constituent quark in a meson, a confining string is elongated and one would observe a pair creation of quark and anti-quark and the string breaking, resulting in two mesons. If one does so for a baryon, three string junction will be seen. A lattice QCD simulation of a bound state of three heavy quarks clearly shows a Y-junction of three confining strings [3–5]. More generally,  $N$  strings join at a junction called a baryon vertex in an  $SU(N)$  Yang-Mills theory. In string theory, confining strings

are identified with fundamental strings [6, 7]. Recently, confining strings are also proposed as cosmic strings [8].

On the other hand, Faddeev and Niemi proposed that glueballs can be represented by knotted strings [9]. To this end, they proposed by using the so-called Cho-Faddeev-Niemi or Cho-Duan-Ge-Faddeev-Niemi-Shabanov decomposition [10–16] (for a review, see Ref. [17]) that  $SU(2)$  Yang-Mills theory is reduced to the Faddeev-Skyrme model, an  $O(3)$  nonlinear sigma model with a four derivative term [18, 19].<sup>1</sup> The target space is  $S^2$  and topological lumps supported by the second homotopy group  $\pi_2(S^2) \simeq \mathbb{Z}$  are identified with confining strings. A straight string was discussed in Refs. [21]. Furthermore, this model admits Hopfions topologically characterized by  $\pi_3(S^2) \simeq \mathbb{Z}$ , which are closed lump strings [22–26], see Refs. [27, 28] for a review. Faddeev and Niemi proposed that these Hopfions can be identified with glueballs.

More realistic case for QCD is the gauge group  $G = SU(3)$ . For the gauge group  $G = SU(N)$ , the decomposition results in a flag manifold [11, 14, 17]

$$F_{N-1} \simeq SU(N)/U(1)^{N-1}. \quad (1.1)$$

The flag manifold sigma models have been recently studied in various contexts in high energy physics and condensed matter physics [29–46], see Ref. [47] for a review: spin chains [29, 30, 38, 39, 44], flag manifold sigma model on  $\mathbb{R} \times S^1$  [35], anomaly and topological  $\theta$  term [36, 45], world-sheet theories of composite non-Abelian vortices [48, 49], and a non-Abelian vortex lattice [50]. The flag manifold sigma models admit several types of topological lumps because of the second homotopy group

$$\pi_2(F_{N-1}) \simeq \pi_1[U(1)^{N-1}] \simeq \mathbb{Z}^{N-1}. \quad (1.2)$$

Various properties of the topological lumps have been elucidated in Refs. [32, 41, 42, 51, 52]. In our previous paper [52], we exhausted Bogomol’nyi-Prasad-Sommerfield (BPS) lumps in supersymmetric Kähler flag sigma models [53–58] and determined their moduli space in terms of the moduli matrix [59–63]. When we regard the flag manifold sigma model as a low-energy theory of the  $SU(N)$  Yang-Mills theory along the line of Faddeev and Niemi [17], Hopfions in the  $F_2$  Faddeev-Skyrme model were discussed in Ref. [43]. In this case, to justify the  $F_2$  Faddeev-Skyrme model as a certain low-energy theory of the  $SU(3)$  Yang-Mills theory, the model should admit an  $N$  string junction, which is the main target of this paper.

In this paper, we show that a stable string junction is indeed present in the flag manifold sigma model with a four derivative term and a potential term. We construct a three-string junction of a Y-shape in the  $F_2 \simeq SU(3)/U(1)^2$  sigma model, which could be relevant for the  $SU(3)$  Yang-Mills theory. More specifically, in this paper, for the purpose to simulate a three-string junction elongated to infinity in  $\mathbb{R}^3$ , we compactify the space to a torus  $T^3$  with twisted boundary conditions, so that one can perform numerical simulations in a finite box, and sheets of crystals composed of the string junctions are numerically constructed. The most important aspect of numerical simulations for the construction is choosing a

---

<sup>1</sup>However, there is also an objection to this claim [20].

topologically correct initial state, prepared using a BPS solution in a Kähler  $F_2$  nonlinear sigma model.

This paper is organized as follows. In Sec. 2 we define the  $F_{N-1}$  Faddeev-Skyrme model. In Sec. 3, we present BPS lump solutions in the  $F_2$  sigma model based on Ref. [52]. In Sec. 4, we numerically construct a stable string junction of Y-shape in the  $F_2$  sigma model on a three dimensional torus  $T^3$ . Sec. 5 is devoted to a summary and discussion. In Appendix A, we give a relation between the parametrizations of the model used in this paper and the original one by Faddeev and Niemi. In Appendix C, we give some details of our numerical calculations.

## 2 $F_{N-1}$ Faddeev-Skyrme model

In this section, we present the model and provide an overview of the topological lumps in the model.

### 2.1 The model

The model we consider in this paper is a 3+1 dimensional theory called the  $F_{N-1}$  Faddeev-Skyrme model, defined by the Lagrangian

$$-\mathcal{L} = \sum_{i=1}^N \left( \frac{f^2}{4} \text{tr} [\partial_\mu P_i \partial^\mu P_i] + \frac{1}{8g^2} F_{\mu\nu}^i F^{i,\mu\nu} \right) + V, \quad (2.1)$$

with the Minkowski metric convention  $\eta_{\mu\nu} = \text{diag}(-1, 1, 1, 1)$ . The first term is the  $F_{N-1}$  sigma model, the second term with four derivatives is called the Skyrme term, and the last term is a potential. The Skyrme term and the potential  $V$  are introduced to avoid a subtle problem on the stability of string junctions (see Sec. 4). The Skyrme term was present in the proposal of Faddeev and Niemi [14]. See Appendix A for the equivalence between the model in Eq. (2.1) and one used by Faddeev and Niemi [14] in which a potential is not considered.

The target manifold  $F_{N-1}$  is described by a set of  $N$  projection matrices  $\{P_i | i = 1, 2, \dots, N\}$  satisfying

$$P_i = (P_i)^\dagger, \quad P_i P_j = \delta_{ij} P_i, \quad \sum_{i=1}^N P_i = \mathbf{1}_N, \quad \text{tr} [P_i] = 1. \quad (2.2)$$

We also define reference projection matrices  $p_i$  as

$$(p_i)_b^a = \delta_{ia} \delta_{ib}. \quad (2.3)$$

Using this  $p_i$ , the set of  $\{P_i\}$  can always be expressed with a unitary matrix  $U \in \text{U}(N)$  as

$$P_i = U^\dagger p_i U \quad \text{for } i = 1, 2, \dots, N, \quad (2.4)$$

where there exists a gauge redundancy of  $\text{U}(1)^N$  acting on  $U$  as

$$U \sim U' = e^{i\Theta} U \quad \text{with} \quad \Theta = \sum_{i=1}^N \theta_i p_i \quad \theta_i \in \mathbb{R}. \quad (2.5)$$

Related to this gauge redundancy, a (composite) gauge field  $A_\mu^i$  and its field strength  $F_{\mu\nu}^i$  are defined as

$$A_\mu^j \equiv i \text{tr} [p_j \partial_\mu U U^\dagger], \quad F_{\mu\nu}^j \equiv \partial_\mu A_\nu^j - \partial_\nu A_\mu^j = -i \text{tr} [P_j [\partial_\mu P_j, \partial_\nu P_j]], \quad (2.6)$$

respectively. In the following, we set the potential term as

$$V = \frac{\mu^2}{4} \sum_{i=1}^N \text{tr} [(p_i - P_i)^2]. \quad (2.7)$$

This potential explicitly breaks the  $U(N)$ -flavor symmetry to  $U(1)^N$  and hence the fluctuations around the vacuum  $U = \mathbf{1}$  have the mass  $\mu/f$ . In addition to the unbroken  $U(1)^N$  symmetry, this model has an  $S_N$  symmetry which permutes the projection matrices  $P_i \leftrightarrow P_j$ .<sup>2</sup> This  $S_N$  symmetry is particular for the model in Eq. (2.1) and does not exist in the  $F_{N-1}$  flag sigma model with more general coefficients, given in Appendix B.

## 2.2 Topological lump strings

Here, we discuss topological lumps corresponding to the second homotopy group  $\pi_2(F_{N-1}) \simeq \mathbb{Z}^{N-1}$  in Eq. (1.2). According to the topological charges, the topological sectors can be classified by the following topological invariant

$$\mathbf{m} = (m_1, m_2, \dots, m_N) : \quad m_j \equiv \frac{1}{4\pi i} \int_\Sigma dx^\mu \wedge dx^\nu F_{\mu\nu}^j \in \mathbb{Z}, \quad (2.8)$$

where  $\Sigma$  is a two-dimensional plane embedded into the base space. Note that this topological invariant has  $N - 1$  degrees of freedom since it must satisfy the constraint

$$\sum_{i=1}^N m_i = 0 \quad \left( \because \sum_{i=1}^N F_{\mu\nu}^i = 0 \right). \quad (2.9)$$

This topological invariant guarantees the existence of string-like topological solitons, which are orthogonal to the plane  $\Sigma$ . Among such string-like objects, an elementary one carries a charge

$$\mathbf{m} = \mathbf{m}^{\langle i, j \rangle} \equiv (0, \dots, 0, \overset{i}{+1}, 0, \dots, 0, \overset{j}{-1}, 0, \dots), \quad (2.10)$$

We call the string-like object with this topological charge  $\langle i, j \rangle$ -string. Each string has a direction: for example, a  $\langle j, i \rangle$ -string is a  $\langle i, j \rangle$ -string extending in the opposite direction. Thus, a pair of parallel  $\langle i, j \rangle$ - and  $\langle j, i \rangle$ -strings can be annihilated:

$$\mathbf{m}^{\langle i, j \rangle} + \mathbf{m}^{\langle j, i \rangle} = \mathbf{0}. \quad (2.11)$$

The composite state of an  $\langle i, j \rangle$ - and  $\langle j, k \rangle$ -strings orthogonal to the plane  $\Sigma$  has the same topological charge with an  $\langle i, k \rangle$ -string:

$$\mathbf{m}^{\langle i, j \rangle} + \mathbf{m}^{\langle j, k \rangle} = \mathbf{m}^{\langle i, k \rangle}. \quad (2.12)$$

---

<sup>2</sup>An element  $\sigma$  of  $S_N$  acts on the unitary matrix  $U$  as  $\mathcal{P}_\sigma^{-1} U \mathcal{P}_\sigma$  with the permutation matrix  $\mathcal{P}_\sigma$ .

All elementary strings have the same tensions thanks to the  $S_N$  symmetry in our model. Therefore, a single  $\langle i, k \rangle$ -string is energetically more stable than two separated  $\langle i, j \rangle$ - and  $\langle j, k \rangle$ -strings.

Based on these facts, it is quite natural to expect that three  $\langle i, j \rangle$ -,  $\langle j, k \rangle$ - and  $\langle k, i \rangle$ -strings extending from three directions meet at a single point and form a string junction as illustrated in Fig. 1. Due to the balance of forces, all three angles between the strings in this junction should be  $2\pi/3$ . The aim of this paper is to show that this configuration indeed exists as a stable solution of the equation of motion.

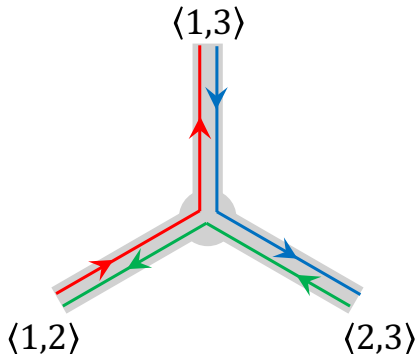


**Figure 1.** Schematic picture of a string junction in the  $N = 3$  case.

### 3 BPS lump solutions as initial configurations

In this section, we prepare initial configurations for iterative numerical simulations to construct a string junction solution discussed in the next section. In the numerical process, the topology of the configuration remains unchanged. Therefore, the initial configuration should have the correct topology to lead to the string junction. To obtain an initial configuration which is topologically equivalent to the string junction, we use BPS string solutions in a Kähler flag manifold sigma model [53–58] without the Skyrme term and the potential term ( $1/g^2 = \mu^2 = 0$ ). Here, we provide an overview the construction of a general BPS solution composed of a  $\langle 1, 2 \rangle$ -lump and a  $\langle 2, 3 \rangle$ -lump in the Kähler flag manifold sigma model.

#### 3.1 Non-Kähler and Kähler $F_{N-1}$ sigma models

Here, we consider the general  $F_{N-1}$  sigma model. The general  $F_{N-1}$  sigma model has  $N(N-1)/2$  parameters as shown in Appendix B. In an  $N$ -dimensional subspace of the parameter space, the model takes the form of  $N$  copies of the  $\mathbb{C}P^{N-1}$  sigma model with some constraints

$$-\mathcal{L}_{\sigma\text{-model}} = \sum_{i=1}^N \frac{r_i}{2} \text{tr} [\partial_\mu P_i \partial^\mu P_i] = \sum_{i=1}^N r_i K_{\text{FS}}(w_i, w_i^\dagger) \quad \text{with} \quad P_i = \frac{w_i^\dagger w_i}{|w_i|^2}. \quad (3.1)$$

Here  $w_i \in \mathbb{C}^N \setminus \{0\}$  ( $i = 1, 2, \dots, N$ ) are row vectors representing the homogeneous coordinates with the equivalence relation  $w_i \sim \lambda_i w_i$  ( $\lambda_i \in \mathbb{C} \setminus \{0\}$ ). They are not independent and must satisfy the orthogonality constraints

$$w_i \cdot w_j^\dagger = 0 \quad \text{for } j \neq i. \quad (3.2)$$

$K_{\text{FS}}$  is the kinetic term with the Fubini-Study metric

$$K_{\text{FS}}(w, w^\dagger) \equiv \frac{1}{|w|^2} \partial^\mu w \left( \mathbf{1} - \frac{w^\dagger w}{|w|^2} \right) \partial_\mu w^\dagger, \quad w \in \mathbb{C}^N \setminus \{0\}. \quad (3.3)$$

The coefficients  $r_i$  ( $i = 1, \dots, N$ ) must satisfy inequalities

$$r_i + r_j > 0 \quad \text{for } j \neq i. \quad (3.4)$$

Note that they can take negative values as long as this inequalities are satisfied. In terms of  $w_i$ , the topological number  $m_i$ , defined in Eq.(2.8), takes the following form seen in the  $\mathbb{C}P^{N-1}$  sigma model:

$$m_i = \frac{1}{2\pi i} \int_\Sigma d \left( \frac{dw_i \cdot w_i^\dagger}{|w_i|^2} \right). \quad (3.5)$$

Now let us focus on the case of the  $F_2$  sigma model ( $N = 3$ ). In this case, Eq. (3.1) is the most general case because  $N(N-1)/2 = 3$  for  $N = 3$ . Note that  $F_2$  is a complex manifold with three inequivalent complex structures. For each choice of the complex structure,  $F_2$  becomes a Kähler manifold by setting one of  $r_i$  to be zero. To express BPS solutions, it is convenient to use the complex coordinates  $\{\phi_1, \phi_2, \phi_3\}$ <sup>3</sup> such that  $w_i$  are given as

$$w_1 \sim (1, \phi_3, \phi_2^+), \quad w_2 \sim (-\phi_3^*, 1, \phi_1'), \quad w_3 \sim (-\phi_2^-)^*, -\phi_1^*, 1) \quad (3.6)$$

where  $\phi_i^*$  stands for the complex conjugate of  $\phi_i$  and

$$\phi_2^\pm \equiv \phi_2 \pm \frac{1}{2} \phi_3 \phi_1, \quad \phi_1' \equiv \frac{\phi_1 - \phi_3^* \phi_2^-}{1 + (\phi_2^+)^* \phi_2}, \quad \phi_3' \equiv \frac{\phi_3 + \phi_1^* \phi_2^+}{1 + \phi_2^+ (\phi_2^-)^*}. \quad (3.7)$$

We can confirm that if one of the parameters  $r_i$  is set to zero, the target manifold becomes a Kähler manifold, otherwise it is not a Kähler manifold. Note that if two of  $r_i$  are set to zero, the target space reduces to  $\mathbb{C}P^2$ .

<sup>3</sup>The complex coordinates  $\{\phi_1, \phi_2, \phi_3\}$  are the parameters contained in the coset matrix as

$$U = \hat{h}^{-1} e^\Phi, \quad \Phi = \begin{pmatrix} 0 & \phi_3 & \phi_2 \\ 0 & 0 & \phi_1 \\ 0 & 0 & 0 \end{pmatrix},$$

where  $U$  is the unitary matrix appearing in Eq.(2.4) and  $\hat{h}$  is the lower triangular matrix which can be determined from  $\hat{h} \hat{h}^\dagger = e^\Phi e^{\Phi^\dagger}$  up to  $U(1)$ <sup>3</sup>.

### 3.2 BPS lumps in the $F_2$ sigma model on $T^2$

Here, we consider strings parallel to the  $x_2$ -axis, which can be viewed as lump solutions localized on the perpendicular 2D plane. We set  $r_2 = 0$  to obtain a Kähler  $F_2$  sigma model admitting BPS lump solutions. In this case, there is no interaction between  $\langle 1, 2 \rangle$ -lumps and  $\langle 2, 3 \rangle$ -lumps. BPS lump solutions are given by holomorphic maps from  $\mathbb{C}$  to  $F_2$  which are represented by meromorphic functions  $(\phi_1(z), \phi_2(z), \phi_3(z))$  of  $z = x_1 + ix_3 \in \mathbb{C}$ .

In the numerical analysis in the next section, it is more convenient to take the basis space to be a torus  $T^2$  rather than the complex plane  $\mathbb{C}$ . Therefore, we take  $\Sigma = T^2$  as the base space.

Let us construct a single BPS lump solution on  $T^2$  by embedding a single  $\mathbb{C}P^1$  lump solution into one of the complex coordinates  $\{\phi_1, \phi_2, \phi_3\}$  of  $F_2$ . A single  $\mathbb{C}P^1$  BPS lump solution is given by a meromorphic function with a single pole (and a single zero). However, all doubly periodic meromorphic functions must have at least two poles (and two zeros) in their fundamental domains. To obtain a single BPS lump solution, let us define  $T^2$  as  $T^2 = \mathbb{C}/\sim$  with  $z \sim z + pL_1 + iqL_3$  ( $p, q \in \mathbb{Z}$ ) by dividing the fundamental domain into two domains and allowing twisted periodicity on  $\{\phi_1, \phi_2, \phi_3\}$  as

$$(\phi_1(z + L_1), \phi_2^\pm(z + L_1), \phi_3(z + L_1)) = (+\phi_1(z), -\phi_2^\pm(z), -\phi_3(z)), \quad (3.8)$$

$$(\phi_1(z + iL_3), \phi_2^\pm(z + iL_3), \phi_3(z + iL_3)) = (-\phi_1(z), -\phi_2^\pm(z), +\phi_3(z)). \quad (3.9)$$

To construct solutions, it is convenient to use the Jacobi's elliptic functions  $\text{sn}(u), \text{sc}(u)$  and  $\text{sd}(u)$ , which have different twisted periodicity given by

$$(\text{sc}(u + 2K), \text{sd}(u + 2K), \text{sn}(u + 2K)) = (+\text{sc}(u), -\text{sd}(u), -\text{sn}(u)), \quad (3.10)$$

$$(\text{sc}(u + 2iK'), \text{sd}(u + 2iK'), \text{sn}(u + 2iK')) = (-\text{sc}(u), -\text{sd}(u), +\text{sn}(u)), \quad (3.11)$$

where  $K$  is the complete elliptic integral of the first kind

$$K(k) = \int_0^{\frac{\pi}{2}} \frac{d\theta}{\sqrt{1 - k^2 \sin^2 \theta}}, \quad K'(k) = K(\sqrt{1 - k^2}). \quad (3.12)$$

Setting the elliptic modulus  $k$  so that  $K(k)/K'(k) = L_1/L_3$ , we can find  $L_* \in \mathbb{R}_{>0}$  such that  $K = L_1/(2L_*)$  and  $K' = L_3/(2L_*)$ . Then, by identifying the coordinates as  $u = z/L_*$ , we can show that each of  $(\text{sn}(u)^{-1}, \text{sc}(u)^{-1}, \text{sd}(u)^{-1})$  is a function that satisfies the twisted boundary conditions (3.8)-(3.9) and has a single pole at  $z = 0$  on  $T^2$ . Therefore, using these functions, we can write down single BPS lump solutions.

The general solution for a single  $\langle 1, 2 \rangle$ -lump is given by

$$\phi_3 = \frac{c_3}{\text{sn}(u - u_3)}, \quad \phi_2^\pm = \phi_1 = 0 \quad \text{with} \quad \mathbf{m} = \mathbf{m}^{(1,2)} \equiv (1, -1, 0), \quad (3.13)$$

where  $\phi_3$  has only one pole at  $u = u_3$ . Similarly, the general solution for a single  $\langle 2, 3 \rangle$ -lump is given by

$$\phi_1 = \frac{c_1}{\text{sc}(u - u_1)}, \quad \phi_2^\pm = \phi_3 = 0 \quad \text{with} \quad \mathbf{m} = \mathbf{m}^{(2,3)} \equiv (0, 1, -1). \quad (3.14)$$

Here,  $c_1$  and  $c_3$  are dimensionless moduli parameters. The quantity  $|c_i|L_*$  roughly gives the size of each lump. We assume that  $|c_i|$  is sufficiently smaller than 1 so that the energy density profile of each lump is localized around  $u = u_i$  (the poles of  $\phi_i$ ).<sup>4</sup>

Next, let us consider composite states of  $\langle 1, 2 \rangle$  and  $\langle 2, 3 \rangle$ -lumps carrying charge  $\mathbf{m} = \mathbf{m}^{(1,2)} + \mathbf{m}^{(2,3)}$ . Eq.,(3.5) implies that in order to have topological charges  $\mathbf{m} = \mathbf{m}^{(1,2)} + \mathbf{m}^{(2,3)}$ ,  $(\phi_3, \phi_2^+)$  and  $(\phi_1, \phi_2^-)$  should each have only one pole at  $u = u_3$  and  $u = u_1$ , respectively. Therefore, the general solution is given by<sup>5</sup>

$$\begin{aligned}\phi_3 &= \frac{c_3}{\text{sn}(u - u_3)}, & \phi_2^+ &= \frac{c_1 c_3}{\text{sc}(u_3 - u_1)} \frac{1}{\text{sd}(u - u_3)}, \\ \phi_1 &= \frac{c_1}{\text{sc}(u - u_1)}, & \phi_2^- &= \frac{c_1 c_3}{\text{sn}(u_3 - u_1)} \frac{1}{\text{sd}(u - u_1)}.\end{aligned}\quad (3.15)$$

By setting  $c_1 = \epsilon c_2$ ,  $c_3 = \epsilon c_2$  and  $u_3 - u_1 = \epsilon^2 c_2$  and taking the limit  $\epsilon \rightarrow 0$ , we find that the above solution for the composite state becomes that for the  $\langle 1, 3 \rangle$ -lump as

$$\phi_2^\pm = \frac{c_2}{\text{sd}(u - u_1)}, \quad \phi_3 = \phi_1 = 0 \quad \text{with} \quad \mathbf{m} = \mathbf{m}^{(1,3)} = (1, 0, -1). \quad (3.16)$$

The existence of the continuous deformation from the  $\langle 1, 2 \rangle$ ,  $\langle 2, 3 \rangle$ -lump composite to the  $\langle 1, 3 \rangle$ -lump clearly indicates that there are no topological obstacles in constructing the string junction illustrated in Fig. 1.

## 4 Numerical solution of string junctions

In this section, we construct a numerical solution of string junctions. We go back to the original Lagrangian of the  $F_2$  model of  $N = 3$  with the  $\mathbb{Z}_3$  symmetry (the model with  $r_1 = r_2 = r_3 = f^2/2$ ) and turn on the Skyrme and potential terms.

### 4.1 Initial configuration and boundary condition

Our goal in this paper is to construct a numerical solution for a string junction illustrated in Fig. 1. To this end, we take the following strategy depicted in Fig. 2. We take a torus  $T^3$  as the base space to clarify the situation in numerical calculations. First, we prepare a pair of  $\langle 1, 2 \rangle$  and  $\langle 2, 3 \rangle$ -strings on the torus so that they form skew lines and nearly intersect each other, as illustrated in the left panel of Fig. 2. Starting from this configuration as an initial condition, we perform a numerical optimization to reduce the energy of the configuration. Then, the two strings will stick together in the middle, producing a  $\langle 1, 3 \rangle$ -string with a pair

<sup>4</sup>Conversely, if  $|c_i|$  is sufficiently larger than 1, we observe an object of size  $|c_i|^{-1}L_*$  localized around zero of  $\phi_i$ .

<sup>5</sup>Here the coefficients in the above  $\phi_2^\pm$  are uniquely determined as follows. The poles of  $\phi_2^+$  and  $\phi_2^-$  are located at the different points, although  $\phi_2^\pm$  are not independent of each other and must satisfy a relation

$$0 = f(u) \equiv \phi_2^-(u) - \phi_2^+(u) + \phi_3(u)\phi_1(u).$$

Therefore, the coefficients in  $\phi_2^\pm$  must be determined so that the two poles in  $f(u)$  cancel out. Once the coefficients are determined in this way,  $f(u)$  becomes a constant function due to the property of elliptic functions, and furthermore, the twisted periodicity of  $f(u)$  automatically requires that  $f(u) = 0$ .

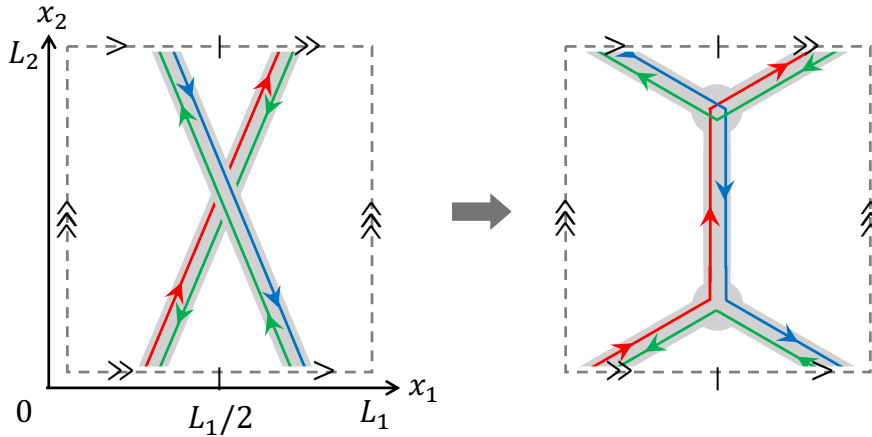


**Figure 2.** Schematic picture of a pair formation of string junctions with an intersection of two strings through numerical optimization.

of the string junctions. As the energy decreases, the length of the  $\langle 1, 3 \rangle$ -string increases further until the angles between all the strings at the junction points become  $2\pi/3$ . The energy is expected to be minimized to reach a solution of the form illustrated in the right panel of Fig. 2. The two types of junctions appearing here are related to each other by spatial rotation and complex conjugation.<sup>6</sup>

More specifically, as the initial configuration, we choose the configuration given in Eq. (3.15) at arbitrary constant  $x_2$  surfaces, set  $c_1 = c_3 = 1/2$  and give the  $x_2$ -dependence to the parameters  $u_1, u_3$  as

$$\begin{aligned} u_3 &= u_3(x_2) \equiv \frac{1}{L_*} \left( \frac{L_1}{4} + \frac{L_1}{2L_2} x_2 + i \left( \frac{L_3}{2} + \delta \right) \right), \\ u_1 &= u_1(x_2) \equiv \frac{1}{L_*} \left( \frac{3L_1}{4} - \frac{L_1}{2L_2} x_2 + i \left( \frac{L_3}{2} - \delta \right) \right), \end{aligned} \quad (4.1)$$

where  $\delta$  is a small constant introduced to avoid a singularity due to intersection of the strings. Here  $u_3(x_2)$  and  $u_1(x_2)$  satisfy  $u_3(x_2 + L_2) = u_3(x_2) + K$ ,  $u_1(x_2 + L_2) = u_1(x_2) - K$ .

On the base space  $T^3$ , we impose the following twisted periodic boundary condition on the projection matrices  $P_i$ :

$$P_i(x_1 + L_1, x_2, x_3) = U_1^\dagger P_i(x_1, x_2, x_3) U_1, \quad U_1 = \text{diag}(-1, 1, 1), \quad (4.2)$$

$$P_i(x_1, x_2, x_3 + L_3) = U_3^\dagger P_i(x_1, x_2, x_3) U_3, \quad U_3 = \text{diag}(1, 1, -1), \quad (4.3)$$

$$P_i \left( x_1 + \frac{L_1}{2}, x_2 + L_2, x_3 \right) = P_i(x_1, x_2, x_3), \quad (4.4)$$

so that this periodicity is consistent with the initial condition given in Eqs. (3.15) and (4.1).

Under this setting, the lengths of the  $\langle 1, 2 \rangle$  and  $\langle 2, 3 \rangle$  strings in the fundamental domain should be  $L_1/\sqrt{3}$  and that of the  $\langle 1, 3 \rangle$ -string becomes  $L_2 - L_1/(2\sqrt{3})$ .

<sup>6</sup>Here, a string is represented by parallel and opposite arrows, but their spatial ordering is merely for the convenience of the drawing and has no physical meaning. Therefore, the twisting of the arrows around the upper junction in the right panel of Fig. 2 has no physical meaning.

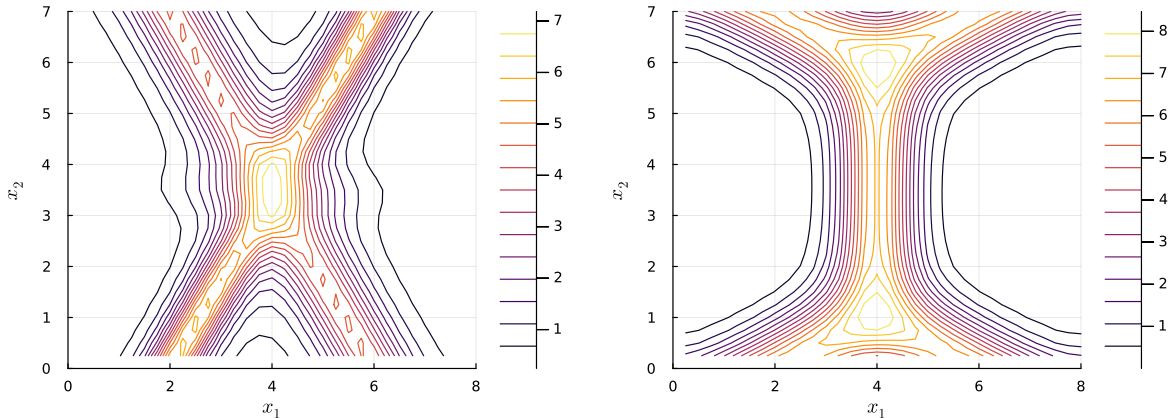


**Figure 3.** Energy densities at the  $x_3 = L_3/2$  cutting plane. The left panel is for the initial state, and the right panel is for the final state of the numerical simulation with  $(L_1, L_2, L_3) = (8, 7, 5)$  and  $a = 1/4$ .

## 4.2 Numerical results

Before considering a string junction, let us briefly describe the basic data of the component lump solution. In the case with  $1/g = \mu = 0$ , the configurations of single lump given in Eqs. (3.13), (3.14) and (3.16) are still solutions even if  $r_2$  is turned on. There, as a result of scale invariance, a flat direction (zero mode) corresponding to the size moduli  $|c_i|$  appears on the configuration space. In the lattice calculations, however, due to the finite lattice spacing, this flat direction  $|c_i|$  is slightly tilted toward the origin of  $c_i$ . Thus, during numerical optimization, the lump size shrinks toward zero and eventually the configurations break down when the lump becomes smaller than the lattice spacing. Therefore, we need to make both of the two parameters,  $1/g$  and  $\mu$ , to be finite to numerically obtain stable lump solutions. With the two parameters, the lump size takes a value roughly estimated to be on the order of  $1/\sqrt{\mu g}$  by the scaling argument.

A set of the values of the parameters for our numerical simulations is

$$f^2 = 1, \quad \frac{1}{g^2} = 1, \quad \mu^2 = 1, \quad (4.5)$$

and the size of the torus is chosen as follows:

$$(L_1, L_2, L_3) = \frac{n}{4} \times (8, 7, 5), \quad \text{with } n = 3, 4, 5, 6. \quad (4.6)$$

Here,  $L_2/L_1 = 7/8$  is chosen to be a rational number close to  $\sqrt{3}/2$ , where the lengths of the three types of strings are approximately equal within the fundamental domain of  $T^3$ .

In these parameter settings, we numerically construct a configuration for a pair of the string junctions, which is our objective in this paper. We conducted numerical simulations using the steepest descent method with a finite difference approximation where the number of lattice points is  $7560 (= 24 \times 21 \times 15) - 483840 (= 96 \times 84 \times 60)$ , and the lattice spacing is

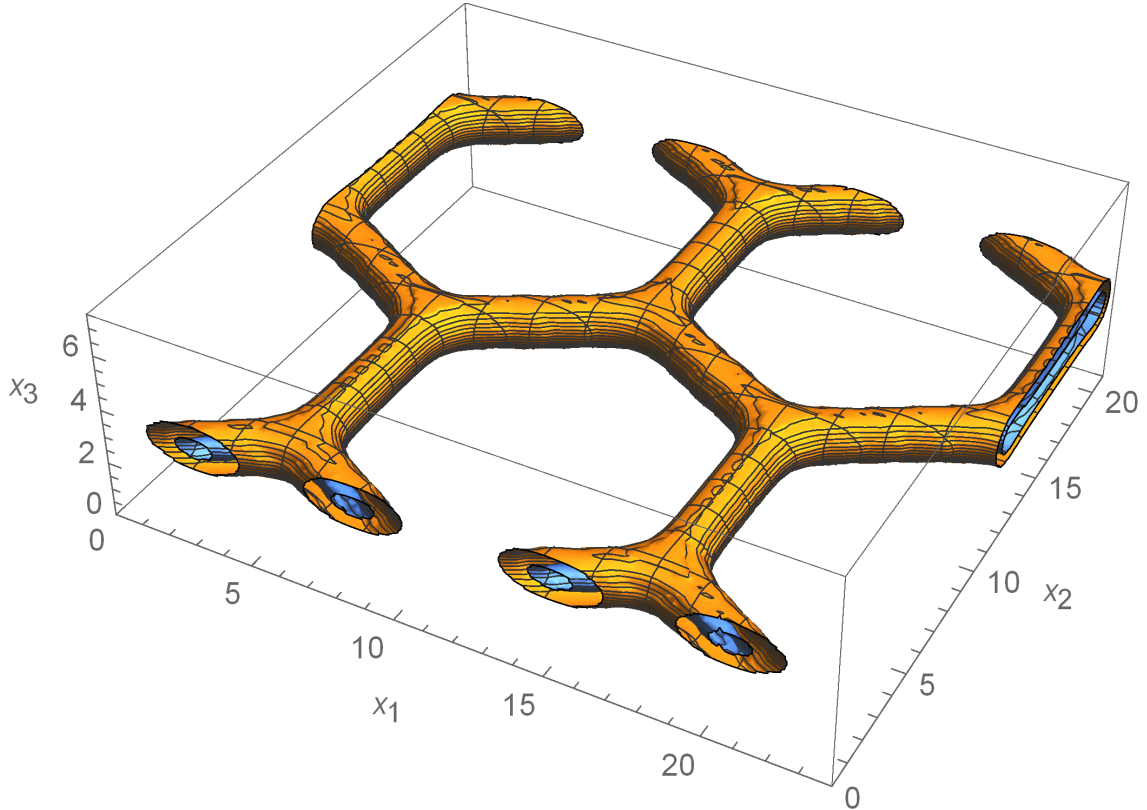


**Figure 4.** The surface contour of  $\rho = 8$  (Orange) and  $\rho = 16$  (Blue) in the energy density  $\rho$  for a net composed of the string junctions in the case with  $(L_1, L_2, L_3) = (12, 10.5, 7.5)$  and  $a = 1/8$ .

taken as either  $a = 1/4$  or  $a = 1/8$ . A detailed description of our numerical method is given in Appendix C. As the result of the numerical optimizations with the initial configuration given in Eqs. (3.15) and (4.1), we obtain the final converged configuration shown in Figs. 3 and 4, in which the energy density  $\rho$  is depicted.

We also study the  $L_i$  dependence of the total energy to remove a possible dependence on situational settings such as the twisted periodic boundary condition we take, as discussed in detail in Appendix C.

## 5 Summary and Discussion

We have numerically constructed a three-string junction of Y-shape in the  $F_2$  sigma model with the four derivative Skyrme and potential terms with a typical set of parameters in the system. The introduction of a potential term stabilizes the strings and thus the string junction is expected to always be stable in the system with an arbitrary set of parameters, independent of the lattice spacing and the periods of the base space  $T^3$ . To eliminate the effects caused by the finite periods of the torus and the finite lattice spacing, we have investigated the  $a$ -dependence and the  $L_i$ -dependence of the string junction. In the large volume limit, it reduces to the junction in  $\mathbb{R}^3$ .

The model taken in this paper has a dimensionless parameter  $\mu/(gf^2)$  which is eventually taken to be 1 for the numerical calculations. Furthermore, we can choose a different type of a four-derivative term and a potential term. Details of the numerical results for the string junction will depend on such choices, however, it is expected that no drastic changes will occur.

Here we address possible future directions and discussion. The original proposal by Faddeev and Niemi is that glueballs are described by Hopfions. Thus far Hopfions in the  $F_2$  Faddeev-Skyrme model was discussed only in Ref. [43]. Therefore, one of possible future directions is to construct Hopfions with junctions and to compare them with glueballs in SU(3) Yang-Mills theory.

Although we have concentrated on a three-string junction in the  $F_2$  nonlinear sigma model, the model itself was defined for general flag manifold  $F_N$ . In the case of the  $F_3$  nonlinear sigma model, we may show that a four-string junction of tetrapod-shape exists using the same manner we took in this paper.

In this paper, we have used BPS strings in the  $F_2$  sigma model just as an initial configuration for numerical simulations. Whether there is a model admitting a BPS string junction is actually an open question. The flag sigma model itself does not admit BPS string junctions. From a supersymmetric point of view, 1/4 BPS equations for string junctions are proposed [64–66] (see also Ref. [67]) but no explicit solution is available. Thus, we expect that there is a supersymmetric theory of any modification of the flag sigma model admitting a BPS string junction.

Cosmological consequences of confining strings as cosmic strings in pure Yang-Mills theory were studied in detail [8], and thus similar analysis could be performed for strings in the flag sigma models. In particular, two strings with different topological charges do not reconnect in their collision. Fig. 2 in fact shows a production of a string stretched between two strings after a collision of these strings with different topological charges.<sup>7</sup> Therefore, a string network is formed in this model, giving an impact on cosmology.

Note Added: While preparing the draft of this paper, we are aware of the paper [69] discussing the string junction in QCD in ArXiv, in which the stability condition of a junction is discussed in terms of a junction mass. It is an important future problem that the junction mass that we obtained in this paper (the right figure of Fig. 5 in Appendix C) is compared with their condition.

## Acknowledgments

YA would like to thank Nobuyuki Sawado and Keisuke Wada. This work is supported in part by JSPS KAKENHI [Grants No. JP23KJ1881 (YA), No. JP21K03558 (TF) and No. JP22H01221 (MN)], the WPI program “Sustainability with Knotted Chiral Meta Matter (SKCM<sup>2</sup>)” at Hiroshima University.

---

<sup>7</sup>A similar phenomenon is known to happen for a collision of two non-commutative strings [68]. Unlike such a case, this occurs even Abelian strings in this paper.

## A Parametrization of the Lagrangian

Faddeev and Niemi conjectured that the  $F_{N-1}$  Faddeev-Skyrme model describes the low-energy limit of  $SU(N)$  Yang-Mills theory. In terms of their parametrization, the Lagrangian (2.1) can be written as

$$-\mathcal{L} = \sum_{a=1}^{N-1} \left( \frac{f^2}{2} \text{tr} [\partial_\mu n_a \partial^\mu n_a] + \frac{1}{g^2} \mathcal{F}_{\mu\nu}^a \mathcal{F}^{a\mu\nu} + \mu^2 \text{tr} [h_a (h_a - n_a)] \right), \quad (\text{A.1})$$

where  $h_a = \frac{1}{2} \lambda_{a(a+2)}$  is the basis of the Cartan subalgebra of  $su(N)$  and the color direction fields  $n_a$  are defined as

$$n_a = U^\dagger h_a U, \quad (\text{A.2})$$

with the  $SU(N)$  matrix  $U$ . The tensor  $\mathcal{F}_{\mu\nu}^a$  are the coefficient of the Kirillov symplectic two-forms defined as

$$\mathcal{F}_{\mu\nu}^a = -\frac{i}{2} \sum_{b=1}^{N-1} \text{tr} [n_a [\partial_\mu n_b, \partial_\nu n_b]]. \quad (\text{A.3})$$

In this appendix, we derive the Lagrangian (2.1) from Eq. (A.1).

In addition to the basis of the Cartan subalgebra of  $su(N)$ , we introduce  $h_N = \frac{1}{\sqrt{2N}} \mathbf{1}$ . The basis satisfies the orthonormal condition

$$\text{tr} [h_a h_b] = \frac{1}{2} \delta_{ab}. \quad (\text{A.4})$$

We decompose them in terms of the diagonal singleton matrices  $p_i$  as

$$h_a = \sum_{i=1}^N \nu_a^i p_i \quad (\text{A.5})$$

with real constants  $\nu_a^i$ . The orthonormalizing condition (A.4) implies that the vectors  $(\nu_a^1, \nu_a^2, \dots, \nu_a^N)$  for  $a = 1, 2, \dots, N$  form an orthogonal basis of  $\mathbb{R}^N$  with the length  $1/\sqrt{2}$ . Therefore, the matrix  $\nu$  is orthogonal, and we find

$$\sum_{a=1}^N \nu_a^i \nu_a^j = \frac{\delta_{ij}}{2}, \quad \sum_{i=1}^N \nu_a^i \nu_b^i = \frac{\delta_{ab}}{2}. \quad (\text{A.6})$$

From Eq. (A.5), we can decompose the color direction fields  $n_a$  in terms of the projectors  $P_i$  as

$$n_a = \sum_{i=1}^N \nu_a^i P_i. \quad (\text{A.7})$$

Substituting it into the first term in Eq. (A.1), we obtain

$$\begin{aligned} \sum_{a=1}^{N-1} \text{tr} [\partial_\mu n_a \partial^\mu n_a] &= \sum_{a=1}^N \text{tr} [\partial_\mu n_a \partial^\mu n_a] \\ &= \sum_{a=1}^N \nu_a^i \nu_a^j \text{tr} [\partial_\mu P_i \partial^\mu P_j] \\ &= \frac{1}{2} \sum_{i=1}^N \text{tr} [\partial_\mu P_i \partial^\mu P_i] \end{aligned} \quad (\text{A.8})$$

where we have used  $\partial_\mu n_N = 0$  because of  $n_N = h_N$ . Similarly, we can write

$$\begin{aligned}
\mathcal{F}_{\mu\nu}^a &= -\frac{i}{2} \sum_{b=1}^N \text{tr} [n_a [\partial_\mu n_b, \partial_\nu n_b]] \\
&= -\frac{i}{2} \sum_{b=1}^N \sum_{j,k,l=1}^N \nu_a^j \nu_b^k \nu_b^l \text{tr} [P_j [\partial_\mu P_k, \partial_\nu P_l]] \\
&= -\frac{i}{4} \sum_{j,k=1}^N \nu_a^j \text{tr} [P_j [\partial_\mu P_k, \partial_\nu P_k]] .
\end{aligned} \tag{A.9}$$

Now, we have an identity for  $i \neq j, j \neq k, k \neq l$  of the form

$$\text{tr} [P_i \partial_\mu P_j \partial_\nu P_k] = \text{tr} [p_i [p_j, U \partial_\mu U^\dagger] [p_k, U \partial_\nu U^\dagger]] = 0 , \tag{A.10}$$

which is implied by  $p_i p_j = \delta_{ij} p_j$ . Using the identity, we obtain

$$\begin{aligned}
\mathcal{F}_{\mu\nu}^a &= -\frac{i}{4} \sum_{j=1}^N \nu_a^j \left\{ \text{tr} [P_j [\partial_\mu P_j, \partial_\nu P_j]] + \sum_{k \neq j} \text{tr} [P_j [\partial_\mu P_k, \partial_\nu P_k]] \right\} \\
&= -\frac{i}{4} \sum_{j=1}^N \nu_a^j \left\{ \text{tr} [P_j [\partial_\mu P_j, \partial_\nu P_j]] + \text{tr} [P_j [\sum_{k \neq j} \partial_\mu P_k, \sum_{l \neq j} \partial_\nu P_l]] \right\} \\
&= -\frac{i}{2} \sum_{j=1}^N \nu_a^j \text{tr} [P_j [\partial_\mu P_j, \partial_\nu P_j]] \\
&= \frac{1}{2} \sum_{j=1}^N \nu_a^j F_{\mu\nu}^j
\end{aligned} \tag{A.11}$$

where we have used  $\sum_{i=1}^N \partial_\mu P_j = 0$ . Therefore, we find that the Skyrme term, the second term in Eq. (A.1), can be cast into the form

$$\begin{aligned}
\sum_{a=1}^{N-1} \mathcal{F}_{\mu\nu}^a \mathcal{F}^{a\mu\nu} &= \sum_{a=1}^N \mathcal{F}_{\mu\nu}^a \mathcal{F}^{a\mu\nu} \\
&= \frac{1}{4} \sum_{a=1}^N \sum_{i,j=1}^N \nu_a^i \nu_a^j F_{\mu\nu}^i F^{j\mu\nu} \\
&= \frac{1}{8} \sum_{i=1}^N F_{\mu\nu}^i F^{i\mu\nu} .
\end{aligned} \tag{A.12}$$

In addition, the potential term can be written as

$$\begin{aligned}
\sum_{a=1}^{N-1} \text{tr} [h_a(h_a - n_a)] &= \sum_{a=1}^N \text{tr} [h_a(h_a - n_a)] \\
&= \sum_{a=1}^N \sum_{i,j=1}^N \nu_a^i \nu_a^j \text{tr} [p_i(p_j - P_j)] \\
&= \frac{1}{2} \sum_{i=1}^N \text{tr} [p_i(p_i - P_i)] \\
&= \frac{1}{4} \sum_{i=1}^N \text{tr} [(p_i - P_i)^2]. \tag{A.13}
\end{aligned}$$

Summarizing the results in Eqs. (A.8), (A.12), and (A.13), we find that the Lagrangian in Eq. (A.1) is equivalent to the one in Eq. (2.1) which we have studied in this paper.

## B $F_{N-1}$ sigma model with general coefficients

In this appendix we introduce the most general form of the  $F_{N-1}$  sigma model. The model can maximally possess  $N(N-1)/2$  parameters as

$$-\mathcal{L}_{\sigma\text{-model}} = -\frac{1}{2} \sum_{j=2}^N \sum_{i=1}^{j-1} f_{ij} \text{tr} [\partial_\mu P_i \partial^\mu P_j]. \tag{B.1}$$

This general model returns to the original one by setting  $f_{ij} = f^2$  for all  $i, j$ . Here the coefficient  $f_{ij} = f_{ji}$  must be positive definite. This can be confirmed as follows. Since  $F_{N-1}$  is a homogeneous complex manifold, we only need to examine the neighborhood of the origin. Substituting a unitary matrix  $U \approx \mathbf{1} + X$  with an anti-Hermitian matrix  $X$  to the projection matrices  $P_i = U^\dagger p_i U$  and taking quadratic terms in the Lagrangian, we find that

$$-\mathcal{L}_{\sigma\text{-model}} \approx \sum_{j=2}^N \sum_{i=1}^{j-1} f_{ij} |\partial_\mu X^i_j|^2, \tag{B.2}$$

which shows that  $f_{ij}$  must be positive definite; if it meets this condition, any value is acceptable. Here, an  $\langle i, j \rangle$ -string remains to be a solution under this deformation to the general  $F_{N-1}$  sigma model, because it is a solution of the  $F_1 \simeq \mathbb{C}P^1$  sigma model embedded into the  $F_{N-1}$  one. Note that the solution might be unstable as a saddle point.

In the absence of the Skyrme and potential terms ( $1/g^2 = \mu^2 = 0$ ), the  $\langle i, j \rangle$ -string is a BPS solution whose tension is given by

$$2\pi f_{ij} \tag{B.3}$$

if and only if  $f_{ij} \leq f_{ik} + f_{kj}$  for all  $k \neq i, j$  [52]. If  $f_{ij} < f_{ik} + f_{kj}$ , an  $\langle i, j \rangle$ -string is energetically more stable than a composite state of  $\langle i, k \rangle$ - and  $\langle k, j \rangle$ -strings. If  $f_{ij} > f_{ik} + f_{kj}$ ,

the  $\langle i, j \rangle$ -string is unstable and will separate into  $\langle i, k \rangle$ - and  $\langle k, j \rangle$ -strings. In the case with  $f_{ij} = f_{ik} + f_{kj}$ , there is no interaction between the  $\langle i, k \rangle$ - and  $\langle k, j \rangle$ -strings, and actually a composite state of them at any relative distance is a BPS state, which is exactly what is discussed in Sec 3.

By setting  $f_{ij} = r_i + r_j$  with introducing  $N$  parameters  $\{r_i\}$ , the above general model reduces to a sum of  $N$  copies of the  $\mathbb{C}P^{N-1}$  sigma model given in Eq.(3.1), where a set  $\{r_i\}$  must satisfy

$$r_i + r_j > 0 \quad \text{for } i \neq j. \quad (\text{B.4})$$

The  $N = 3$  case is special where parameter space of Eq.(B.1) and one in Eq.(3.1) are equivalent since

$$\begin{aligned} f_{ij} &= r_i + r_j \\ \Leftrightarrow r_1 &= \frac{1}{2}(f_{12} + f_{13} - f_{23}), \quad r_2 = \frac{1}{2}(f_{12} + f_{23} - f_{13}), \quad r_3 = \frac{1}{2}(f_{13} + f_{23} - f_{12}), \end{aligned} \quad (\text{B.5})$$

and thus the model given in Eq.(3.1) is the most general.

## C Numerical calculation

In this appendix, we describe some details of our numerical calculations.

### C.1 $F_{N-1}$ on the lattice

Let us discretize the system by taking a  $d$ -dimensional Euclidean lattice  $\Gamma$  as the base space, where the action is a function whose variables are a set of unitary matrices  $U_{\vec{x}} \in \text{U}(N)$  defined at each point  $\vec{x} \in \Gamma$  as,

$$S^o = a^d \sum_{\vec{x} \in \Gamma} \sum_{i=1}^N \left[ \frac{f^2}{2a^2} \sum_{j=1, (j \neq i)}^N \sum_{\mu=1}^d \text{tr} [P_i^{\vec{x}+\vec{\mu}} P_j^{\vec{x}}] + \frac{1}{8g^2} \sum_{\mu, \nu=1}^d (F_{\mu\nu}^{i, \vec{x}})^2 + \frac{\mu^2}{4} \text{tr} [(P_i^{\vec{x}} - p_i)^2] \right] \quad (\text{C.1})$$

with the projection matrices  $P_i^{\vec{x}} = U_{\vec{x}}^\dagger p_i U_{\vec{x}}$ , the lattice spacing  $a$  and  $\vec{\mu}$  defined to point to an adjacent lattice point as  $(\vec{\mu})^\nu = a\delta_\mu^\nu$ . The field strength  $f_{\mu\nu}^{i, \vec{x}}$  is defined as

$$F_{\mu\nu}^{i, \vec{x}} \equiv \frac{1}{a^2} \text{Im} \text{tr} [P_i^{\vec{x}} P_i^{\vec{x}+\vec{\mu}} P_i^{\vec{x}+\vec{\mu}+\vec{\nu}} P_i^{\vec{x}+\vec{\nu}}] = F_{\mu\nu}^i \left( \vec{x} + \frac{\vec{\mu} + \vec{\nu}}{2} \right) + \mathcal{O}(a^2). \quad (\text{C.2})$$

Note that, to define an energy density  $\rho_{\vec{x}}$  at  $\vec{x} \in \Gamma$  used in Figs.3 and 4, the values at the relevant adjacent lattice points need to be averaged since the difference and the field strength on  $\Gamma$  are defined on the links and the plaquettes of  $\Gamma$ , respectively.

In order to deal with the variation with respect to the unitary matrices, it is convenient to introduce Lagrange multipliers  $\lambda_{\vec{x}}$  which are  $N$ -th order Hermitian matrices defined at each  $\vec{x} \in \Gamma$  and to add terms to the original action  $S^o$  as follows:

$$S = S^o - a^d \sum_{\vec{x} \in \Gamma} \text{tr} [\lambda_{\vec{x}} (U_{\vec{x}}^\dagger U_{\vec{x}} - \mathbf{1}_N)], \quad \text{with } \lambda_{\vec{x}}^\dagger = \lambda_{\vec{x}}, \quad (\text{C.3})$$

where the matrix  $U_{\vec{x}}$  is not restricted to unitary. Here, thanks to the  $U(1)^N$  gauge symmetry,  $U_{\vec{x}}$  does not appear explicitly in  $S^0$  and the function  $S^0$  is written in terms of the matrices  $P_i^{\vec{x}}$ . Therefore, we can define a variation of  $S^0$  with respect to  $P_i^{\vec{x}}$  as

$$Q_i^{\vec{x}} \equiv \frac{\delta' S^0}{\delta' P_i^{\vec{x}}} = (Q_i^{\vec{x}})^\dagger, \quad \Leftrightarrow \quad \delta S^0(\{P_i^{\vec{x}}\}) \equiv a^d \sum_{\vec{x} \in \Gamma} \sum_{i=1}^N \text{tr} [\delta P_i^{\vec{x}} Q_i^{\vec{x}}], \quad (\text{C.4})$$

where each  $P_i^{\vec{x}}$  is treated as if it were an arbitrary Hermitian matrix unrelated to each other, and  $\delta'$  means a variation under that manner.<sup>8</sup>

Under the above preparations, we can derive a variation of the action as

$$\delta S = a^d \sum_{\vec{x} \in \Gamma} \text{tr} [i U_{\vec{x}}^{-1} \delta U_{\vec{x}} \mathcal{H}_{\vec{x}} + \text{h.c.}] \quad (\text{C.5})$$

with the matrix  $\mathcal{H}_{\vec{x}}$  defined by

$$\mathcal{H}_{\vec{x}} \equiv -i \left( \sum_{i=1}^N Q_i^{\vec{x}} P_i^{\vec{x}} - \lambda_{\vec{x}} \right) = \frac{i}{2} \sum_{i=1}^N [P_i^{\vec{x}}, Q_i^{\vec{x}}], \quad (\text{C.6})$$

where we require that  $\mathcal{H}_{\vec{x}}$  is Hermitian,  $\mathcal{H}_{\vec{x}} = \mathcal{H}_{\vec{x}}^\dagger$ . This requirement gives an equation solved for the Lagrange multiplier as,

$$\lambda_{\vec{x}} = \frac{1}{2} \sum_{i=1}^N \{P_i^{\vec{x}}, Q_i^{\vec{x}}\} \quad (= (\lambda_{\vec{x}})^\dagger). \quad (\text{C.7})$$

Since there are  $N$  identities on  $\mathcal{H}_{\vec{x}}$ ,  $\text{tr} [P_i^{\vec{x}} \mathcal{H}_{\vec{x}}] = 0$  under the unitary condition  $U_{\vec{x}}^\dagger U_{\vec{x}} = \mathbf{1}$ , the number of independent equations in  $\mathcal{H}_{\vec{x}} = 0$  is  $N(N-1)$  which is just the dimension of  $F_{N-1}$ . Therefore,  $\mathcal{H}_{\vec{x}} = 0$  is nothing more than the equation of motion in this system.

## C.2 Numerical method and some results

To obtain numerical solutions to  $\mathcal{H}_{\vec{x}} = 0$ , we apply a gradient method, steepest descent, to this system. We set each step of the numerical calculation on the set of the unitary matrices  $\{U_{\vec{x}} | \vec{x} \in \Gamma\}$  as

$$U_{\vec{x}} \rightarrow U_{\vec{x}}^{(\alpha)} = U_{\vec{x}} e^{i\alpha \mathcal{H}_{\vec{x}}}, \quad \left( P_i^{\vec{x},(\alpha)} = e^{-i\alpha \mathcal{H}_{\vec{x}}} P_i^{\vec{x}} e^{i\alpha \mathcal{H}_{\vec{x}}} \right), \quad (\text{C.8})$$

with an appropriate step size  $\alpha \in \mathbb{R}_{>0}$ . If we choose a sufficiently small  $\alpha$ , this method ensures that the total energy is always decreasing at each step, because

$$\lim_{\alpha \rightarrow +0} \frac{1}{\alpha} \left[ S(\{P_i^{\vec{x},(\alpha)}\}) - S(\{P_i^{\vec{x}}\}) \right] = -2a^d \sum_{\vec{x} \in \Gamma} \text{tr} \mathcal{H}_{\vec{x}}^2 \leq 0. \quad (\text{C.9})$$

Note that, since  $\mathcal{H}_{\vec{x}}$  is Hermitian, each step of iterations will automatically keep the unitary condition  $U^\dagger U = \mathbf{1}$ , if the initial condition satisfies it.

---

<sup>8</sup>In other words,  $Q_i^{\vec{x}}$  is defined by extending the function  $S^0(\{P_i^{\vec{x}}\})$  by extrapolation outside the domain of definition of  $P_i^{\vec{x}}$ . Strictly speaking this extension and thus the definition of  $Q_i^{\vec{x}}$  are not unique, but there should be no problem with this definition since the introduction of  $Q_i^{\vec{x}}$  is only for notational simplicity.

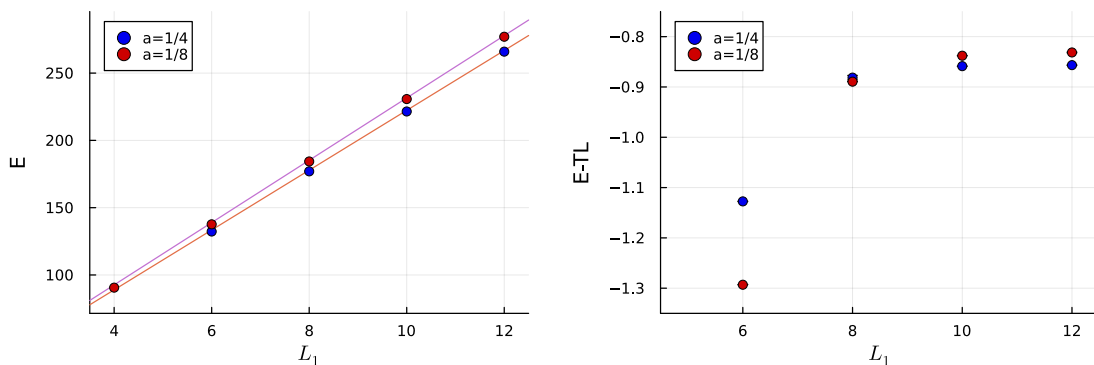


**Figure 5.**  $L_i$ -dependence of total energy of the string junction for each fundamental domain of  $T^3$ , with the lattice spacing  $a = 1/4, 1/8$  and keeping the ratio of the periods,  $L_1 : L_2 : L_3 = 8 : 7 : 5$ .

After enough iterations of the steps in a numerical simulation, the deviation from the solution of the fields  $\phi_i^{\vec{x}}$  decreases exponentially as  $\delta\phi_i^{\vec{x}} \approx \varphi_i^{\vec{x}} e^{-\Delta t}$ , where  $\varphi_i^{\vec{x}}$  is the lightest massive mode around the solution and  $\Delta$  is a certain positive real number related to the mass gap and  $t$  is the relaxation time as the accumulation of  $\alpha$  in each step up to that point. Under the optimization, therefore, that of the total energy  $E$  behaves as  $\delta E \propto e^{-2\Delta t}$  whereas the other observed quantities  $O_a$  behave as  $\delta O_a \propto e^{-\Delta t}$ . Using this knowledge, a faster converging sequence of numbers  $\{\hat{E}_n\}$  can be constructed from the sequence  $\{E_n\}$  obtained by the gradient method as follows,

$$\hat{E}_n \equiv \frac{E_n E_{n-2} - E_{n-1}^2}{E_n + E_{n-2} - 2E_{n-1}}, \quad (\text{C.10})$$

and then the calculation error can be roughly estimated as  $|\hat{E}_n - E_n|$  when the calculation is terminated at a certain  $n$ .<sup>9</sup>

In Sec. 4.2, we applied the gradient method explained above to the construction of the string junctions. The boundary conditions we have adopted here are technical and not essential to the construction of the string junction. In order to estimate and remove the effect of the periodic boundary conditions, we plot the  $L_i$ -dependence of the total energy in Fig. 5 with keeping the ratio  $L_1 : L_2 : L_3 = 8 : 7 : 5$ . In those numerical calculations the termination conditions were set as follows

$$\forall \vec{x} \in \Gamma : \quad \sqrt{\text{tr}[\mathcal{H}_{\vec{x}}^2]} \leq \mathcal{O}(10^{-4}) \quad \text{or} \quad \mathcal{O}(10^{-3}) \quad (\text{C.11})$$

and then calculation errors in the total energy are estimated to be  $|\hat{E}_n - E_n| < 5 \times 10^{-4}$  which can be omitted in Fig. 5. It can be confirmed that these numerical solutions satisfy at least  $\sqrt{\text{tr}[(U_{\vec{x}}^\dagger U_{\vec{x}} - \mathbf{1})^2]} \leq \mathcal{O}(10^{-11})$ , and as explained above, the unitary condition is almost preserved. As can be seen in the left panel of Fig. 5, the linear potentials as contributions

<sup>9</sup>Due to truncation errors from taking the difference, the calculation of  $\hat{E}_n$  requires higher computational accuracy than that of  $E_n$ . Therefore, if the required accuracy for  $\hat{E}_n$  exceed the calculation accuracy, then this estimation does not work well.

from the strings dominate the total energy, where the solid lines are given by

$$T \times \left( \frac{\sqrt{3}}{2} L_1 + L_2 \right) \quad \text{with } T = \begin{cases} 12.7706 & \text{for } a = \frac{1}{4} \\ 13.2993 & \text{for } a = \frac{1}{8} \end{cases} \quad \text{and } L_2 = \frac{7}{8} L_1. \quad (\text{C.12})$$

Here  $T$  is the sting tension and its values are estimated by applying the same method as in Eq.(C.10) to the difference of the total energy  $dE/dL_1$ . In the right panel of Fig. 5, we removed these contributions from the total energy. There, a value obtained in the limit of  $L_1 = \infty$  should be a quantity independent of the boundary conditions. Since the  $a$ -dependence of the total energy should be approximated by a smooth function of  $a^2$ , the total energy in the continuum limit is roughly predictable by extrapolation. For example, a true value of the tension of the lump string with parameters given in Eq. (4.5) is estimated to be  $T \approx 13.5$ .

## References

- [1] Y. Nambu, *Strings, Monopoles and Gauge Fields*, *Phys. Rev. D* **10** (1974) 4262.
- [2] S. Mandelstam, *Vortices and Quark Confinement in Nonabelian Gauge Theories*, *Phys. Rept.* **23** (1976) 245.
- [3] T. T. Takahashi, H. Matsufuru, Y. Nemoto and H. Suganuma, *The Three quark potential in the SU(3) lattice QCD*, *Phys. Rev. Lett.* **86** (2001) 18 [[hep-lat/0006005](#)].
- [4] T. T. Takahashi, H. Suganuma, Y. Nemoto and H. Matsufuru, *Detailed analysis of the three quark potential in SU(3) lattice QCD*, *Phys. Rev. D* **65** (2002) 114509 [[hep-lat/0204011](#)].
- [5] G. S. Bali, *QCD forces and heavy quark bound states*, *Phys. Rept.* **343** (2001) 1 [[hep-ph/0001312](#)].
- [6] R. Donagi and E. Witten, *Supersymmetric Yang-Mills theory and integrable systems*, *Nucl. Phys. B* **460** (1996) 299 [[hep-th/9510101](#)].
- [7] J. Polchinski and M. J. Strassler, *The String dual of a confining four-dimensional gauge theory*, [hep-th/0003136](#).
- [8] M. Yamada and K. Yonekura, *Cosmic strings from pure Yang–Mills theory*, *Phys. Rev. D* **106** (2022) 123515 [[2204.13123](#)].
- [9] L. D. Faddeev and A. J. Niemi, *Knots and particles*, *Nature* **387** (1997) 58 [[hep-th/9610193](#)].
- [10] Y. M. Cho, *A Restricted Gauge Theory*, *Phys. Rev. D* **21** (1980) 1080.
- [11] Y. M. Cho, *Coloered Monopoles*, *Phys. Rev. Lett.* **44** (1980) 1115 [Erratum: *Phys.Rev.Lett.* **44**, 1566 (1980)].
- [12] Y.-S. Duan and M.-L. Ge, *SU(2) Gauge Theory and Electrodynamics with N Magnetic Monopoles*, *Sci. Sin.* **9** (1979) .
- [13] L. D. Faddeev and A. J. Niemi, *Partially dual variables in SU(2) Yang-Mills theory*, *Phys. Rev. Lett.* **82** (1999) 1624 [[hep-th/9807069](#)].
- [14] L. D. Faddeev and A. J. Niemi, *Partial duality in SU(N) Yang-Mills theory*, *Phys. Lett. B* **449** (1999) 214 [[hep-th/9812090](#)].

- [15] L. D. Faddeev and A. J. Niemi, *Decomposing the Yang-Mills field*, *Phys. Lett. B* **464** (1999) 90 [[hep-th/9907180](#)].
- [16] S. V. Shabanov, *Yang-Mills theory as an Abelian theory without gauge fixing*, *Phys. Lett. B* **463** (1999) 263 [[hep-th/9907182](#)].
- [17] K.-I. Kondo, S. Kato, A. Shibata and T. Shinohara, *Quark confinement: Dual superconductor picture based on a non-Abelian Stokes theorem and reformulations of Yang-Mills theory*, *Phys. Rept.* **579** (2015) 1 [[1409.1599](#)].
- [18] L. D. Faddeev, *Quantization of Solitons*, in *Preprint IAS Print-75-QS70 (IAS, PRINCETON)*, 6, 1975.
- [19] L. D. Faddeev, *Some Comments on the Many Dimensional Solitons*, *Lett. Math. Phys.* **1** (1976) 289.
- [20] J. Evslin and S. Giacomelli, *A Faddeev-Niemi Solution that Does Not Satisfy Gauss' Law*, *JHEP* **04** (2011) 022 [[1010.1702](#)].
- [21] L. A. Ferreira, J. Jaykka, N. Sawado and K. Toda, *Vortices in the Extended Skyrme-Faddeev Model*, *Phys. Rev. D* **85** (2012) 105006 [[1112.1085](#)].
- [22] R. A. Battye and P. M. Sutcliffe, *Knots as stable soliton solutions in a three-dimensional classical field theory.*, *Phys. Rev. Lett.* **81** (1998) 4798 [[hep-th/9808129](#)].
- [23] R. A. Battye and P. Sutcliffe, *Solitons, links and knots*, *Proc. Roy. Soc. Lond. A* **455** (1999) 4305 [[hep-th/9811077](#)].
- [24] J. Hietarinta and P. Salo, *Faddeev-Hopf knots: Dynamics of linked unknots*, *Phys. Lett. B* **451** (1999) 60 [[hep-th/9811053](#)].
- [25] J. Hietarinta and P. Salo, *Ground state in the faddeev-skyrme model*, *Phys. Rev. D* **62** (2000) 081701.
- [26] M. Kobayashi and M. Nitta, *Torus knots as Hopfions*, *Phys. Lett. B* **728** (2014) 314 [[1304.6021](#)].
- [27] E. Radu and M. S. Volkov, *Existence of stationary, non-radiating ring solitons in field theory: knots and vortons*, *Phys. Rept.* **468** (2008) 101 [[0804.1357](#)].
- [28] Y. M. Shnir, *Topological and Non-Topological Solitons in Scalar Field Theories*. Cambridge University Press, 7, 2018.
- [29] D. Bykov, *Haldane limits via Lagrangian embeddings*, *Nucl. Phys. B* **855** (2012) 100 [[1104.1419](#)].
- [30] D. Bykov, *The geometry of antiferromagnetic spin chains*, *Commun. Math. Phys.* **322** (2013) 807 [[1206.2777](#)].
- [31] D. Bykov, *Integrable properties of sigma-models with non-symmetric target spaces*, *Nucl. Phys. B* **894** (2015) 254 [[1412.3746](#)].
- [32] D. Bykov, *Classical solutions of a flag manifold  $\sigma$ -model*, *Nucl. Phys. B* **902** (2016) 292 [[1506.08156](#)].
- [33] D. Bykov, *Flag manifold  $\sigma$ -models: The  $\frac{1}{N}$ -expansion and the anomaly two-form*, *Nucl. Phys. B* **941** (2019) 316 [[1901.02861](#)].
- [34] D. Bykov, *Flag manifold sigma-models and nilpotent orbits*, *Proc. Steklov Inst. Math.* **309** (2020) 78 [[1911.07768](#)].

- [35] M. Hongo, T. Misumi and Y. Tanizaki, *Phase structure of the twisted  $SU(3)/U(1)^2$  flag sigma model on  $\mathbb{R} \times S^1$* , *JHEP* **02** (2019) 070 [[1812.02259](#)].
- [36] Y. Tanizaki and T. Sulejmanpasic, *Anomaly and global inconsistency matching:  $\theta$ -angles,  $SU(3)/U(1)^2$  nonlinear sigma model,  $SU(3)$  chains and its generalizations*, *Phys. Rev. B* **98** (2018) 115126 [[1805.11423](#)].
- [37] K. Ohmori, N. Seiberg and S.-H. Shao, *Sigma Models on Flags*, *SciPost Phys.* **6** (2019) 017 [[1809.10604](#)].
- [38] M. Lajkó, K. Wamer, F. Mila and I. Affleck, *Generalization of the Haldane conjecture to  $SU(3)$  chains*, *Nucl. Phys. B* **924** (2017) 508 [[1706.06598](#)], [Erratum: Nucl.Phys.B 949, 114781 (2019)].
- [39] K. Wamer, M. Lajkó, F. Mila and I. Affleck, *Generalization of the Haldane conjecture to  $SU(n)$  chains*, *Nucl. Phys. B* **952** (2020) 114932 [[1910.08196](#)].
- [40] A. Smerald and N. Shannon, *Theory of spin excitations in a quantum spin-nematic state*, *Phys. Rev. B* **88** (2013) 184430 [[1307.5131](#)].
- [41] H. T. Ueda, Y. Akagi and N. Shannon, *Quantum solitons with emergent interactions in a model of cold atoms on the triangular lattice*, *Phys. Rev. A* **93** (2016) 021606 [[1511.06515](#)].
- [42] Y. Amari and N. Sawado, *BPS sphalerons in the  $F_2$  nonlinear sigma model*, *Phys. Rev. D* **97** (2018) 065012 [[1711.00933](#)].
- [43] Y. Amari and N. Sawado,  *$SU(3)$  Knot Solitons: Hopfions in the  $F_2$  Skyrme-Faddeev-Niemi model*, *Phys. Lett. B* **784** (2018) 294 [[1805.10008](#)].
- [44] K. Wamer and I. Affleck, *Flag manifold sigma models from  $SU(n)$  chains*, *Nucl. Phys. B* **959** (2020) 115156 [[2007.01912](#)].
- [45] R. Kobayashi, Y. Lee, K. Shiozaki and Y. Tanizaki, *Topological terms of  $(2+1)d$  flag-manifold sigma models*, *JHEP* **08** (2021) 075 [[2103.05035](#)].
- [46] I. Takahashi and Y. Tanizaki, *Sigma-model analysis of  $SU(3)$  antiferromagnetic spins on the triangular lattice*, *Phys. Rev. B* **104** (2021) 235152 [[2109.10051](#)].
- [47] I. Affleck, D. Bykov and K. Wamer, *Flag manifold sigma models:: Spin chains and integrable theories*, *Phys. Rept.* **953** (2022) 1 [[2101.11638](#)].
- [48] M. Eto, T. Fujimori, S. Bjarke Gudnason, Y. Jiang, K. Konishi, M. Nitta et al., *Group Theory of Non-Abelian Vortices*, *JHEP* **11** (2010) 042 [[1009.4794](#)].
- [49] E. Ireson, *General Composite Non-Abelian Strings and Flag Manifold Sigma Models*, *Phys. Rev. Res.* **2** (2020) 013038 [[1908.08499](#)].
- [50] M. Kobayashi, E. Nakano and M. Nitta, *Color Magnetism in Non-Abelian Vortex Matter*, *JHEP* **06** (2014) 130 [[1311.2399](#)].
- [51] C. J. C. Negreiros, *Some remarks about harmonic maps into flag manifolds*, *Indiana University Mathematics Journal* **37** (1988) 617.
- [52] T. Fujimori, M. Nitta and K. Ohashi, *Moduli spaces of instantons in flag manifold sigma models. Vortices in quiver gauge theories*, *JHEP* **02** (2024) 230 [[2311.04508](#)].
- [53] M. Bando, T. Kuramoto, T. Maskawa and S. Uehara, *Structure of Nonlinear Realization in Supersymmetric Theories*, *Phys. Lett. B* **138** (1984) 94.

- [54] M. Bando, T. Kuramoto, T. Maskawa and S. Uehara, *Nonlinear Realization in Supersymmetric Theories*, *Prog. Theor. Phys.* **72** (1984) 313.
- [55] M. Bando, T. Kuramoto, T. Maskawa and S. Uehara, *Nonlinear Realization in Supersymmetric Theories. 2.*, *Prog. Theor. Phys.* **72** (1984) 1207.
- [56] K. Itoh, T. Kugo and H. Kunitomo, *Supersymmetric Nonlinear Realization for Arbitrary Kahlerian Coset Space  $G/H$* , *Nucl. Phys. B* **263** (1986) 295.
- [57] K. Itoh, T. Kugo and H. Kunitomo, *Supersymmetric Nonlinear Lagrangians of Kahlerian Coset Spaces  $G/H$ :  $G = E_6, E_7$  and  $E_8$* , *Prog. Theor. Phys.* **75** (1986) 386.
- [58] M. Nitta, *Auxiliary field methods in supersymmetric nonlinear sigma models*, *Nucl. Phys. B* **711** (2005) 133 [[hep-th/0312025](#)].
- [59] Y. Isozumi, M. Nitta, K. Ohashi and N. Sakai, *All exact solutions of a  $1/4$  Bogomol'nyi-Prasad-Sommerfield equation*, *Phys. Rev. D* **71** (2005) 065018 [[hep-th/0405129](#)].
- [60] M. Eto, Y. Isozumi, M. Nitta, K. Ohashi and N. Sakai, *Instantons in the Higgs phase*, *Phys. Rev. D* **72** (2005) 025011 [[hep-th/0412048](#)].
- [61] M. Eto, Y. Isozumi, M. Nitta, K. Ohashi and N. Sakai, *Moduli space of non-Abelian vortices*, *Phys. Rev. Lett.* **96** (2006) 161601 [[hep-th/0511088](#)].
- [62] M. Eto, K. Konishi, G. Marmorini, M. Nitta, K. Ohashi, W. Vinci et al., *Non-Abelian Vortices of Higher Winding Numbers*, *Phys. Rev. D* **74** (2006) 065021 [[hep-th/0607070](#)].
- [63] M. Eto, Y. Isozumi, M. Nitta, K. Ohashi and N. Sakai, *Solitons in the Higgs phase: The Moduli matrix approach*, *J. Phys. A* **39** (2006) R315 [[hep-th/0602170](#)].
- [64] M. Naganuma, M. Nitta and N. Sakai, *BPS lumps and their intersections in  $N=2$  SUSY nonlinear sigma models*, *Grav. Cosmol.* **8** (2002) 129 [[hep-th/0108133](#)].
- [65] M. Eto, Y. Isozumi, M. Nitta and K. Ohashi,  *$1/2$ ,  $1/4$  and  $1/8$  BPS equations in SUSY Yang-Mills-Higgs systems: Field theoretical brane configurations*, *Nucl. Phys. B* **752** (2006) 140 [[hep-th/0506257](#)].
- [66] S. B. Gudnason, M. Eto and M. Nitta,  *$1/2$ -BPS vortex strings in  $\mathcal{N} = 2$  supersymmetric  $U(1)^N$  gauge theories*, *J. Math. Phys.* **62** (2021) 032304 [[2008.13440](#)].
- [67] M. G. Jackson, *A Note on Cosmic  $(p,q,r)$  Strings*, *Phys. Rev. D* **75** (2007) 087301 [[hep-th/0610059](#)].
- [68] M. Kobayashi, Y. Kawaguchi, M. Nitta and M. Ueda, *Collision Dynamics and Rung Formation of Non-Abelian Vortices*, *Phys. Rev. Lett.* **103** (2009) 115301 [[0810.5441](#)].
- [69] Z. Komargodski and S. Zhong, *The Baryon Junction and String Interactions*, [2405.12005](#).